

ML-Aided Indoor Illumination Estimation for Supercapacitor-Based ZE-IoT with Photovoltaic Energy Harvesting

Amila Perera

Centre for Wireless Communications, University of Oulu, Oulu, Finland
malalgodage.perera@oulu.fi

Marcos Katz

Centre for Wireless Communications, University of Oulu, Oulu, Finland
marcos.katz@oulu.fi

Accurate estimation of indoor illumination is critical for sustaining the operation of battery-free Photovoltaic (PV) Energy-Harvesting (EH) based Zero-Energy Internet of Things (ZE-IoT) nodes. Most of these nodes rely on supercapacitors for energy storage, which offer high cycle life but exhibit low energy density compared to batteries. Consequently, the available runtime depends heavily on the limited optical power density typically found in indoor environments. Using dedicated optical sensors to monitor illumination increases node complexity, raises energy overhead, and is susceptible to noise. To address these challenges, this work proposes a novel Machine Learning (ML) approach that estimates indoor incident illumination on ZE-IoT nodes from supercapacitor voltage variations, thereby eliminating the need for dedicated illumination sensors. For concept evaluation, a Random Forest regressor with Leave-One-Out Cross-Validation (LOO-CV) is employed to infer optical power availability from the supercapacitor's discharge behavior. Experimental validation using a ZE-IoT prototype based on the LIoT platform demonstrates an average estimation error of ± 29.8 lux. By transferring illumination estimation to the network side, the proposed method reduces node complexity, supports energy-constrained operation, and enables proactive outage mitigation in sustainable ZE-IoT deployments.

Note: The final version of this paper has been accepted for presentation at the *IEEE Future Networks World Forum (FNWF) 2025*.

1 Introduction

With the advent of 6G wireless systems, sustainability has become a fundamental design criterion, necessitating advanced strategies for energy-efficient architectures, minimization of environmental impact, and intelligent resource allocation across heterogeneous network components. As a result, Internet of Things (IoT) technologies under future network architectures are becoming increasingly aligned with sustainability, which is recognized as a core Key Performance Indicator (KPI) for 6G networks [1]. Since IoT devices are commonly deployed across large indoor environments such as homes, offices, and industrial facilities, achieving energy efficiency and minimizing maintenance requirements have become essential to ensure long-term, scalable, and environmentally conscious operation. In this context, the Zero-Energy Internet of Things (ZE-IoT) paradigm has emerged as a promising solution for sustainable operation by eliminating electrochemical energy storage components. ZE-IoT devices operate solely on energy harvested from ambient natural or artificial sources, eliminating the need for battery replacement or manual recharging. These devices typically rely on capacitors, supercapacitors, or printed solid-state batteries for energy storage. This significantly reduces energy consumption and carbon emissions, enabling scalable, pervasive, and environmentally sustainable IoT deployments. Furthermore, the approach minimizes maintenance requirements, lowers operational costs, and enhances device recyclability, contributing to the broader sustain-

ability goals of future wireless networks [2, 3]. The recent formation of the "Ambient IoT Alliance" highlights a promising industry-driven direction toward the adoption of self-sustaining, battery-free IoT solutions, further reinforcing the relevance of ZE-IoT technologies in future network ecosystems [4].

Nevertheless, battery-free ZE-IoT designs introduce several challenges that must be addressed for real-world deployment. Typically, such systems are powered by Energy Harvesting (EH) technologies that extract energy from ambient sources, such as light, heat, or vibration. Due to the absence of electrochemical batteries, battery-free ZE-IoT designs often rely on more sustainable electrostatic energy storage elements, such as supercapacitors, which serve as intermediate buffers to manage the fluctuating energy demands of typical IoT operations [5]. However, owing to the high power density characteristics of supercapacitors, their voltage levels are expected to fluctuate significantly, depending on both the EH rate from the source and the energy consumption rate of the node [6].

Technologies such as Light-based IoT (LIoT) represent a class of battery-free ZE-IoT designs that utilize Photovoltaic (PV) EH and Optical Wireless communication (OWC) [7]. In such systems, consistent illumination is essential to ensure that the node can harvest sufficient energy to sustain its operation. However, in real-world indoor deployment scenarios, maintaining consistent illumination is challenging due to the highly dynamic nature of indoor lighting conditions [7]. Insufficient illumination can lead to energy outages at the node level, which must be mitigated to ensure reliable operation. Approaches such as adaptive duty cycling and energy networking have been proposed in the literature to address this issue [7, 8]. However, initiating such mitigation techniques requires mechanisms to evaluate the current illumination level so that the network can assess energy availability and the survivability of the node under prevailing conditions.

Incorporating dedicated sensors to measure illumination levels may increase node design complexity, cost, and energy consumption. Moreover, relying on instantaneous illumination measurements can be unreliable, as nodes may be temporarily exposed to fluctuating lighting conditions such as direct sunlight, artificial light in-

terference, or shading caused by movement or obstructions in the environment. These transient effects can lead to inaccurate energy assessments and result in suboptimal network-level decisions. To address these challenges, Machine Learning (ML)-based energy level prediction techniques have been widely explored in the context of battery state estimation for IoT systems. Among the most commonly used supervised regression algorithms are Linear Regression, Random Forest Regression (RandF), Regression Transformer (RT), Support Vector Regression (SVR), Kernel Ridge Regression (KRR), and Dynamic Treatment Regime (DTR) [9, 10].

Building on these advancements, this paper proposes an ML-assisted illumination estimation approach for LIoT and PV-EH based battery-free ZE-IoT networks. In the proposed method, the illumination level, which reflects the available optical energy in the environment, is estimated at the network side using the capacitor voltage data received from the node. Shifting the estimation process to the network reduces the computational and energy overhead on the node and supports a simplified, energy-efficient node design. Based on the estimated illumination, the network can apply appropriate outage mitigation strategies to improve the operational time of ZE-IoT nodes under varying indoor lighting conditions.

The rest of the paper is organized as follows: Section II discusses the model of the proposed system. Section III describes the implemented prototype system for evaluation. Finally, Section IV presents the results and discussion, followed by conclusions.

2 System model

A typical deployment scenario of battery-free ZE-IoT nodes in an indoor environment is illustrated in Fig. 1. Typically, LIoT nodes consist of integrated PV cells along with circuitry for PV-EH and sensing operations. These nodes may also include indicators and displays tailored to specific application domains such as logistics, retail, or healthcare, functioning as smart tags, containers, or labels [7]. As depicted, Node 1 is positioned closer to the illumination source and receives higher illumination, resulting in increased EH rate. In comparison, Node 2 is located in a region with lower illumination due to

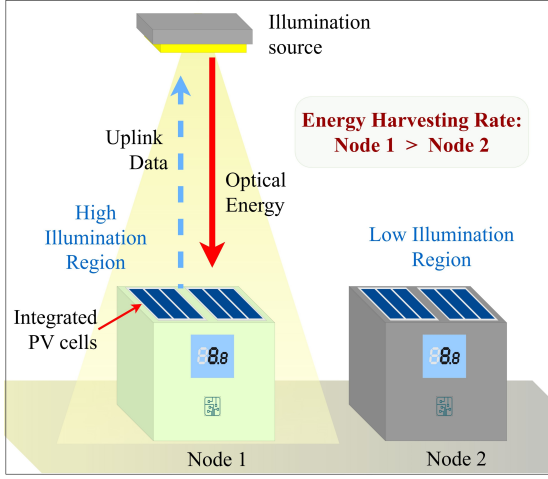


Figure 1: Typical scenario of illumination variation for indoor-deployed PV-EH-based IoT nodes. Nodes exposed to higher illumination levels can harvest energy at increased rates.

placement or shadowing, leading to reduced EH rate. Therefore, the energy accumulation rate in the supercapacitor storage is expected to vary between the two nodes in the scenario. Generally, the energy stored in a supercapacitor can be expressed as [11]:

$$E_{cap} = \frac{1}{2} C_{cap} V_{cap}^2, \quad (1)$$

where E_{cap} denotes the energy stored in the supercapacitor, C_{cap} is the capacitance, and V_{cap} is the voltage across the capacitor. Taking the time derivative of (1) yields the instantaneous rate of change of stored energy:

$$\frac{dE}{dt} = C_{cap} V_{cap} \frac{dV_{cap}}{dt}, \quad (2)$$

where $\frac{dV_{cap}}{dt}$ is the instantaneous rate of change of the capacitor voltage. Alternatively, the rate of change of stored energy can be described by the balance between the harvested power and the consumed power:

$$\frac{dE}{dt} = P_{PV} - P_{load}, \quad (3)$$

where P_{PV} is the power harvested by the PV cells, and P_{load} is the average power consumption of the node. Equating (2) and (3) leads to

$$C_{cap} V_{cap} \frac{dV_{cap}}{dt} = P_{PV} - P_{load}, \quad (4)$$

which describes the voltage variation of the capacitor as a function of the net power flow. Assuming that the capacitor voltage remains ap-

proximately constant within the short sampling window Δt , and denoting the initial voltage at the beginning of the interval as V_{init} , (4) can be expressed as

$$\Delta V_{cap} \approx \frac{P_{PV} - P_{load}}{C_{cap} V_{init}} \Delta t, \quad (5)$$

where ΔV_{cap} is the change in capacitor voltage over the interval Δt , and V_{init} is the initial voltage at the beginning of that interval. The harvested power P_{PV} can be expressed in terms of the optical power density and the PV cell area as

$$P_{PV} = P_d A, \quad (6)$$

where P_d is the incident optical power density on the PV surface, and A is the active area of the PV cell. Substituting (6) into (5) yields the voltage-power-density relationship:

$$\Delta V_{cap} \approx \frac{A P_d - P_{load}}{C_{cap} V_{init}} \Delta t, \quad (7)$$

which relates the capacitor voltage change to the incident optical power. From (7), the relationship between incident optical power and the corresponding voltage change can be observed. Therefore, this expression can be used to estimate the incident optical power, which is analogous to indoor illuminance levels expressed in lux. The sign of ΔV_{cap} in (7) determines the direction of voltage evolution and reflects the balance between harvested and consumed power. Specifically:

- $A P_d > P_{load}$, the harvested power exceeds the load demand, resulting in $\Delta V_{cap} > 0$, and the capacitor voltage gradually increases.
- $A P_d = P_{load}$, the harvested power exactly matches the consumption, yielding $\Delta V_{cap} = 0$, and the capacitor voltage remains stable.
- $A P_d < P_{load}$, the harvested power is insufficient to sustain the load, leading to $\Delta V_{cap} < 0$, and the capacitor voltage decreases over time.

Based on the above power scenarios, the expected voltage variations of a ZE-IoT node using a supercapacitor, under identical initial voltage conditions, are illustrated in Fig. 2. As shown, when the harvested power exceeds the load demand, the capacitor voltage gradually increases

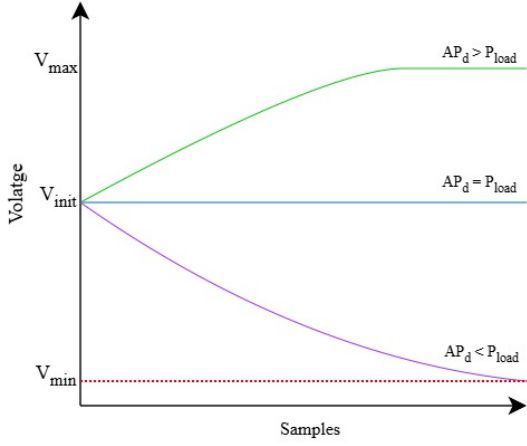


Figure 2: Expected voltage variation scenarios based on the relationship between load power consumption and harvested energy at the node.

and stabilizes near its maximum value. If the harvested power matches the load, the voltage remains steady over time. In contrast, when the harvested power is insufficient to meet the consumption, the capacitor voltage gradually declines toward the minimum threshold, potentially resulting in node outage. In such scenarios, the number of possible transmissions or the duration until the node reaches the turn-off threshold voltage under zero EH conditions can be considered the Worst-Case Scenario (WCS). Therefore, these voltage evolution patterns can be employed to infer the illumination level, which correlates with the harvested optical energy, without the need for direct optical measurements. The overall system model of the proposed approach is depicted in Fig. 3. To implement this estimation, ML-based regression techniques can be employed to map the voltage trends to corresponding illumination levels.

3 Implementation

For the performance evaluation of the concept, a LIoT-based battery-free ZE-IoT prototype platform was used. The platform design was similar to that utilized in previous works [12–14]. The LIoT prototype system consists of a LIoT node, which is the sensor deployed indoors, and an Optical Access Point (OAP), which provides both indoor illumination and OWC for the deployed LIoT nodes.

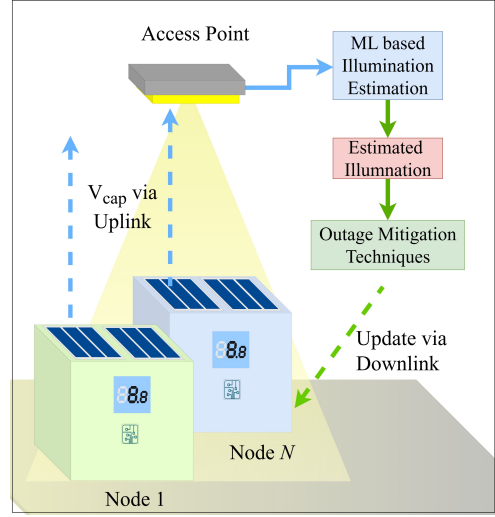


Figure 3: System model of the proposed illumination estimation and outage mitigation concept. A network of battery-free ZE-IoT nodes (from Node 1 to Node N) transmits V_{cap} to the access point via uplink. The network performs ML-based illumination estimation and initiates outage mitigation strategies accordingly, while configuration updates are sent back to the nodes via the downlink.

3.1 Battery-free ZE-IoT node based system

The node featured a TMP36GT9Z analog temperature sensor for sensing and Infrared (IR) transmission for uplink communication. For OWC, RC5 IR protocol was used to encode both the node address and the payload, which included temperature and capacitor voltage readings. The prototype was built around an Arduino Pro Mini (3.3 V, 8 MHz) microcontroller with the onboard LED and voltage regulators disabled for low-power operation. The node structure is shown in Fig. 4. The Energy Harvesting Unit (EHU) of the node was based on the Epishine EK01LEH3-6 evaluation kit, which consisted of an AEM10941 Power Management Integrated Circuit (PMIC) with Maximum Power Point Tracking (MPPT), a CAP-XX GA230F 0.4 F supercapacitor for energy storage, and a TPS62740 DC-DC converter for regulated output. Three Epishine LEH3-50x50-6-10 printed Organic PV (OPV) cells were integrated into the platform to enable multi-directional EH. However, this functionality was not utilized in the evaluation conducted in this work. Capacitor voltage was periodically measured us-

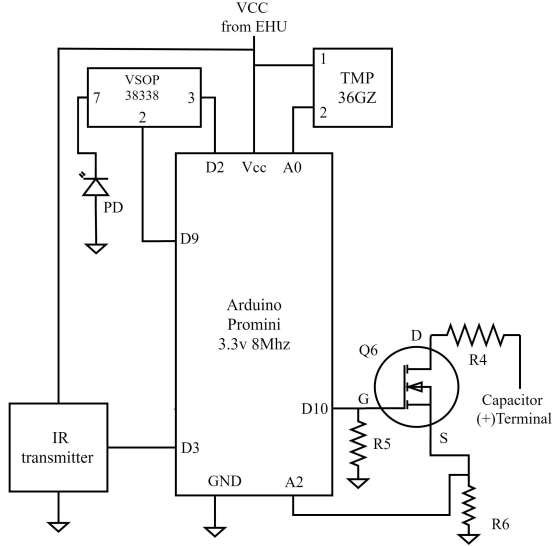


Figure 4: Schematic of the battery-free LLoT ZE-IoT prototype used in the experiments, including the supercapacitor voltage measurement circuit.

ing a MOSFET-controlled path and resistive divider, enabling accurate sampling within the ADC voltage range.

The corresponding OAP of the prototype system consisted of an Arduino Nano microcontroller interfaced with KY-022 optical signal receiver modules. Each module was oriented to enable multi-directional IR signal reception. Upon detecting an IR signal above the module's internal sensitivity threshold, the KY-022 converted it into a Transistor-Transistor Logic (TTL) signal, which was then processed by the Arduino Nano for fast demodulation and decoding. The decoded data were transmitted to a host computer via USB for data collection and analysis. As a variable illumination source, the OAP was equipped with a Chip-on-Board (COB) type cool white LED array, capable of adjusting illumination levels through a controlled power supply.

3.2 ML based evaluation

Given the nonlinear nature of the illumination estimation problem and the limited dataset size due to WCS constraints and prototype limitations, complementing ML-based approach is required for effective modeling. To address this, the use of a RandF Regressor can be proposed for this task. To ensure effective utilization of the available data and enable reliable performance evaluation, Leave-One-Out (LOO) Cross-

Validation (CV) can be adopted. This technique is appropriate for small-sample scenarios, as it systematically uses each data point for testing while training on the remaining samples [10]. In order to evaluate the model's predictive accuracy, Mean Absolute Error (MAE) and the coefficient of determination (R^2 score) can be proposed as the primary performance metrics [9]. The MAE, as defined in (8), quantifies the average magnitude of prediction errors without considering their direction.

$$\text{MAE} = \frac{1}{n} \sum_{i=1}^n |y_i - \hat{y}_i|, \quad (8)$$

The coefficient of determination (R^2), shown in (9), measures the proportion of variance in the actual values that is predictable from the model outputs.

$$R^2 = 1 - \frac{\sum_{i=1}^n (y_i - \hat{y}_i)^2}{\sum_{i=1}^n (y_i - \bar{y})^2}. \quad (9)$$

where, y_i represents the actual observed value, \hat{y}_i denotes the predicted value, \bar{y} is the mean of the actual values, and n is the total number of samples.

4 Performance Evaluation

For the performance evaluation, the LLoT node was initially configured to transmit temperature and supercapacitor voltage values at 30-second intervals. The node was placed 0.6 meters below the OAP, and only the IR uplink channel was utilized for communication. To mitigate possible data losses occurring during transmission, the algorithm was designed to send each data frame three times. The setup arrangement used for obtaining measurements is shown in Fig. 5. The node operated using an internal timer that periodically triggered sensing and data transmission, followed by a transition to deep sleep mode to reduce energy consumption and improve the net EH rate. The power consumption profile of the node was measured using the Nordic Power Profiler Kit II, and the resulting measurement is shown in Fig. 6. According to the graph, the node consumed an average sleep current of 26.67 μA , an active current of 4.48 mA, and a transmission current of 10.15 mA.

To construct the dataset, the LLoT node's supercapacitor was fully charged to establish a con-

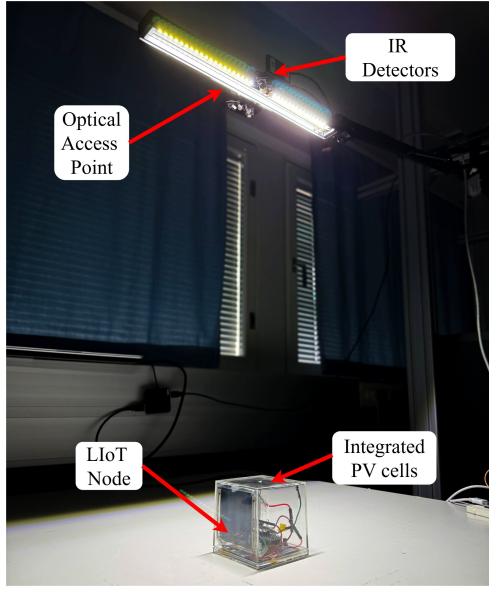


Figure 5: Experimental setup consisting of a battery-free LIoT node and an OAP.

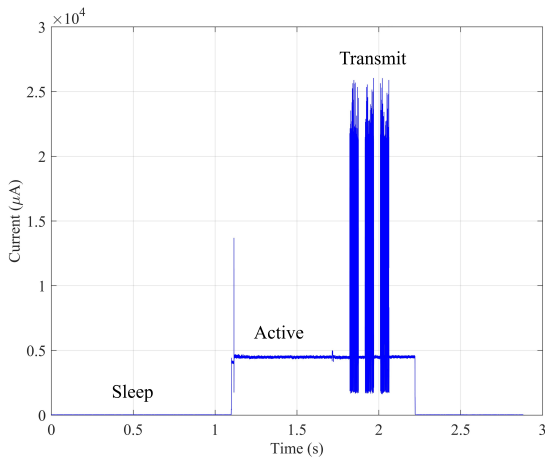


Figure 6: Power profile of the LIoT node consisting Sleep, Active and Transmit stages.

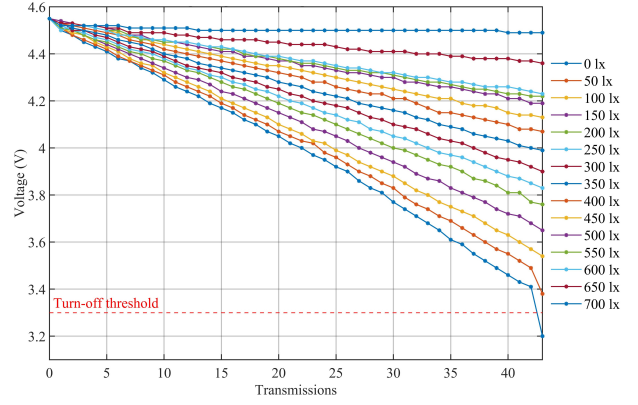


Figure 7: Dataset comprising voltage traces corresponding to a fully charged initial condition under different illumination levels, based on the received uplink data from the node.

sistent initial condition. For illumination measurement, a Chauvin Arnoux CA1110 LED lux meter was used. First, the WCS was evaluated under 0 lux illumination, representing a no EH condition. Under this scenario, the number of successful transmissions until energy depletion was recorded. For all subsequent measurements under varying illumination levels, data collection was limited to the same number of transmission intervals observed in the WCS. This approach ensured a fair and consistent basis for performance comparison across different lighting conditions. The resulting dataset is illustrated in Fig. 7.

According to the dataset, the prototype LIoT node used for the evaluation was able to perform only 43 transmissions under the no-illumination condition before reaching the supercapacitor turn-off voltage threshold, resulting in node outage. In contrast, the voltage profiles under higher illumination levels, particularly those around 700 lux and above, exhibit stabilization toward steady-state values. This indicates that the prototype LIoT node achieves energy autonomy under sufficient lighting conditions, enabling continuous operation without energy depletion.

Due to the approximately linear relationship between the received illumination and the Maximum Power Point (MPP) of the LEH3 OPV cells, the energy storage voltage traces of MPPT-enabled LIoT prototype node exhibit a gradual increase in the EH rate as the illumination level increases. This results in a wider spread in the voltage depletion curves across different

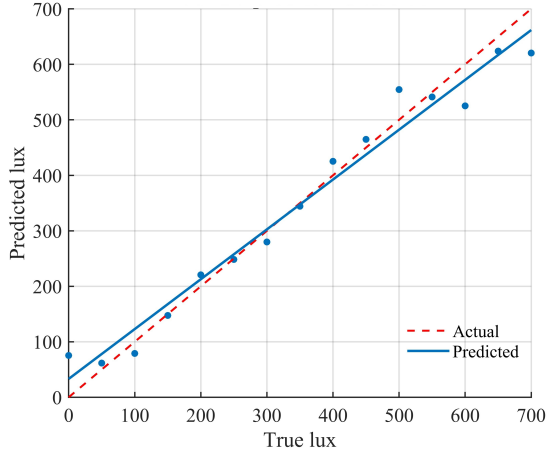


Figure 8: Predicted and actual illumination variation based on RandF regression with LOO-CV.

illumination conditions, providing a distinguishable pattern that can be exploited for ML-based estimation.

4.1 Predicted vs actual lux variation for all samples

For this experiment, all 43 samples corresponding to each illumination level were used to evaluate the model's performance. Fig. 8 illustrates the comparison between the actual and predicted illumination curves. According to the results, the RandF Regressor with LOO-CV, when trained on the full dataset, is able to predict illumination levels that closely match the actual values.

4.2 Performance variation for different number of samples

For this experiment, the number of voltage samples was incremented in steps of 10 to observe the prediction improvement of the model. The resulting performance variation is illustrated in Fig. 9. Based on the results, it can be observed that the MAE decreases as the number of samples increases. According to the graph, when more than 20 samples are used, the prediction accuracy improves by over 30%. When all 43 samples are utilized, the model achieves a MAE of approximately 29.8 lux and an R^2 score of 0.973, indicating strong predictive performance. This suggests that the proposed RandF approach is capable of estimating illumination levels with an average error margin of ± 26.8 lux

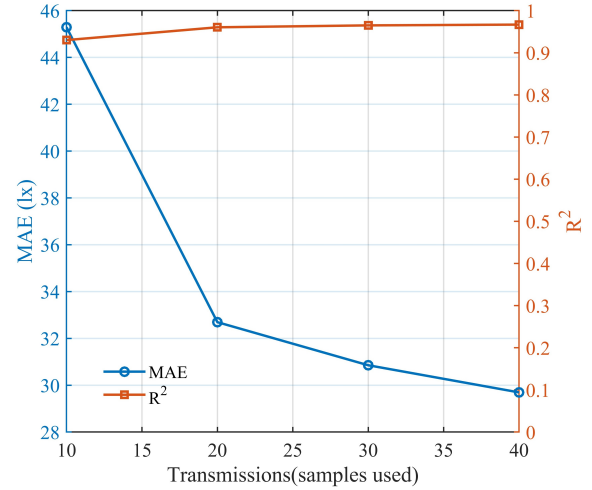


Figure 9: Performance variation with respect to the number of samples, showing corresponding MAE and R^2 metrics.

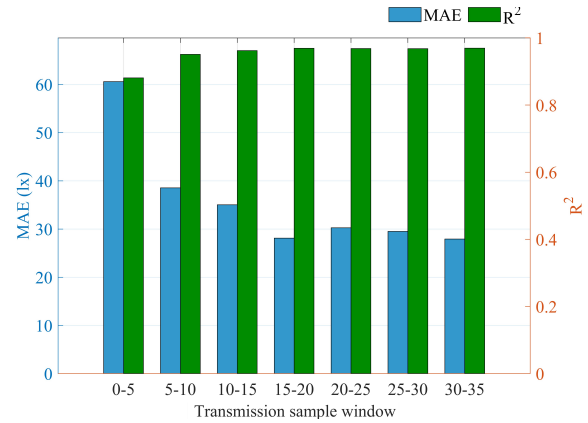


Figure 10: Prediction performance variation across different sliding sample windows, showing the corresponding MAE and R^2 metrics.

based on a sequence of 43 capacitor voltage measurements.

4.3 Performance analysis using moving sample windows

However, in the considered scenario, the system can receive a maximum of 43 transmissions due to energy constraints. Therefore, achieving accurate lux prediction using a minimal number of samples is essential for improving overall system performance. To assess this, a fixed-size sample window of six samples was used and shifted across the dataset to evaluate the impact of window position on the model's prediction accuracy. The obtained results are illustrated in Fig. 10.

As shown, the model achieves better performance when the sampling window covers the

later portions of the transmission sequence. As the sliding window advances toward the latter part of the voltage trace, the model exhibits a noticeable improvement in prediction accuracy. Specifically, the MAE decreases from approximately 60 lux for the 0–5 sample window to around 28 lux for the 30–35 window, while the R^2 score increases from approximately 0.88 to 0.97. This trend is expected, as all voltage traces originate from a common initial condition, with the supercapacitor fully charged to approximately 4.5 V. Consequently, the early samples are nearly identical across different illumination levels and contain limited predictive information. As the discharge progresses, the voltage traces begin to diverge. Under low illumination conditions, the voltage drops more rapidly, while under higher illumination, it remains relatively stable. By the 30–35 sample window, a voltage difference of approximately 0.7 V is observed between the 0 lux and 700 lux cases. This separation in the input space provides the RandF model with more discriminative features, resulting in improved prediction accuracy.

5 Conclusion

This research presents a novel ML-based approach for estimating the availability of optical energy in PV-EH battery-free ZE-IoT nodes. The proposed method enables network-side prediction of indoor illumination conditions, allowing proactive execution of power outage mitigation strategies for nodes operating under energy-deficient environments. The concept was experimentally validated using the LIoT prototype platform, employing RandF regression combined with LOO-CV. While LOO-CV is computationally intensive, it was chosen for this initial study to ensure robust evaluation, and it yielded promising results. The prototype node achieved fully autonomous operation under ambient light levels around 700 lux, utilizing OWC for uplink data transfer. In this study, the evaluation assumed an initial condition of a fully charged supercapacitor. The results demonstrated an average prediction error margin of ± 29.8 lux, indicating the effectiveness of the proposed approach. By offloading illumination estimation to the network side, the proposed method reduces the complexity of ZE-IoT nodes and supports operation under strict energy constraints.

This enables the network to proactively anticipate energy shortages at individual nodes and apply mitigation strategies before outages occur. Moreover, the proposed concept opens new opportunities for indoor environments, such as generating 2D illumination maps to enable intelligent lighting control, contributing to the development of energy-efficient green buildings. As future work, more advanced yet computationally efficient ML models can be investigated to further improve system robustness, including the capability to detect sudden shadowing events without relying on predefined initial conditions.

Acknowledgment

This work was supported by 6G Flagship (Grant Number 369116) funded by the Research Council of Finland, and the SUPERIoT projects. The SUPERIoT project has received funding from the Smart Networks and Services Joint Undertaking (SNS JU) under the European Union’s Horizon Europe research and innovation programme under Grant Agreement No 101096021, including top-up funding by UK Research and Innovation (UKRI) under the UK government’s Horizon Europe funding guarantee. Views and opinions expressed are however those of the authors only and do not necessarily reflect those of the European Union, SNS JU or UKRI. The European Union, SNS JU or UKRI cannot be held responsible for them.

References

- [1] M. A. Uusitalo, P. Rugeland, M. R. Boldi, E. C. Strinati, P. Demestichas, M. Ericson, G. P. Fettweis, M. C. Filippou, A. Gati, M.-H. Hamon, M. Hoffmann, M. Latva-Aho, A. Pärssinen, B. Richerzhagen, H. Schotten, T. Svensson, G. Wikström, H. Wymeersch, V. Ziegler, and Y. Zou, “6G vision, value, use cases and technologies from european 6G flagship project Hexa-X,” *IEEE Access*, vol. 9, pp. 160 004–160 020, 2021.
- [2] T. Khan, S. N. K. Veedu, A. Rácz, M. Afshang, A. Höglund, and J. Bergman, “Toward 6G zero-energy internet of things: Standards, trends, and recent results,”

- IEEE Communications Magazine*, vol. 62, no. 12, pp. 82–88, 2024.
- [3] O. López, R. K. Singh, D.-T. Phan-Huy, E. Katranaras, N. Mazloum, K. Ruttik, R. Jäntti, H. Khan, O. Rosabal, P. Alexias, P. Raghuwanshi, D. Ruiz-Guirola, B. Singh, A. Höglund, D. P. Van, A. Azarbahram, and J. Famaey, “Zero-energy devices for 6G: Technical enablers at a glance,” *IEEE Internet of Things Magazine*, vol. 8, no. 3, pp. 14–22, 2025.
 - [4] Ambient IoT Alliance. (2024) Ambient IoT alliance. <https://www.ambient-iot.org/>. Accessed: August 2025.
 - [5] A. Takacs, G. Loubet, T. Djidjekh, L. Sanogo, and D. Dragomirescu, “Battery-free wireless sensors for IoT applications,” in *2024 15th International Conference on Communications (COMM)*, 2024, pp. 1–6.
 - [6] D. Kularatna-Abeywardana and N. Kularatna, “Supercapacitor energy storage for battery-less, greener IoT networks,” in *2023 IEEE Green Technologies Conference (GreenTech)*, 2023, pp. 160–163.
 - [7] A. Perera, R. Godaliyadda, J. Hakkinen, and M. Katz, “Lighting the way for a sustainable future: Overcoming challenges in light-based IoT and data-energy networking,” *IEEE Communications Magazine*, pp. 1–7, 2025.
 - [8] D. Munir, S. T. Shah, D. M. Mughal, K. H. Park, and M. Y. Chung, “Duty cycle optimizing for WiFi-based IoT networks with energy harvesting,” in *Proceedings of the 12th International Conference on Ubiquitous Information Management and Communication*, ser. IMCOM ’18. New York, NY, USA: Association for Computing Machinery, 2018.
 - [9] J. E. Z. Macias and S. Trilles, “Machine learning-based prediction model for battery levels in IoT devices using meteorological variables,” *Internet of Things*, vol. 25, p. 101109, 2024.
 - [10] Y. Li, C. Zou, M. Berecibar, E. Nanini-Maury, J. C.-W. Chan, P. van den Bossche, J. Van Mierlo, and N. Omar, “Random forest regression for online capacity estimation of lithium-ion batteries,” *Applied Energy*, vol. 232, pp. 197–210, 2018.
 - [11] B. Wang, C. Wang, Z. Wang, H. Xue, and S. Ni, “Adaptive energy estimation for supercapacitor based on a real-time voltage state observer in electric vehicle applications,” *IEEE Transactions on Power Electronics*, vol. 36, no. 7, pp. 7337–7341, 2021.
 - [12] A. Perera, K. Botirov, H. Sallouha, and M. Katz, “ML-aided 2-D indoor positioning using energy harvesters and optical detectors for self-powered light-based IoT sensors,” *IEEE Sensors Journal*, vol. 25, no. 9, pp. 15 958–15 967, 2025.
 - [13] A. Perera, K. Botirov, and M. Katz, “ML-enhanced indoor positioning using photovoltaic cells for light-based internet of things,” in *2024 IEEE Future Networks World Forum (FNWF)*, 2024, pp. 357–364.
 - [14] A. Perera, R. Godaliyadda, and M. Katz, “DE-LIoT: The data-energy networking paradigm for sustainable light-based internet of things,” *arXiv preprint arXiv:2404.14333v1*, 2024.